Extracellular Domains, Transmembrane Segments, and Intracellular Domains Interact To Determine the Cation Selectivity of Na,K- and Gastric H,K-ATPase†

Martin Mense,‡ Vanathy Rajendran,‡ Rhoda Blostein,§ and Michael J. Caplan*,‡

Department of Cellular & Molecular Physiology, Yale University School of Medicine, New Haven, Connecticut 06520-8026, and Departments of Medicine and Biochemistry, McGill University, Montreal, Quebec, Canada H3G 1A4

Received March 19, 2002; Revised Manuscript Received May 31, 2002

ABSTRACT: We have previously reported that three residues of the fourth transmembrane segment (TM4) of the Na,K- and gastric H,K-ATPase α-subunits appear to play a major role in the distinct cation selectivities of these pumps [Mense, M., et al. (2000) *J. Biol. Chem. 275*, 1749−1756]. Substituting these three residues in the Na,K-ATPase sequence with their H,K-ATPase counterparts (L319F, N326Y, T340S) and replacing the TM3−TM4 ectodomain sequence with that of the H,K-ATPase α-subunit result in a pump that exhibits 50% of its maximal ATPase activity in the absence of Na^+ when the assay is performed at pH 6.0. This effect is not seen when the ectodomain alone is replaced. To gain more insight into the contributions of the three residues to establishing the selectivity of these pumps for Na^+ ions versus protons, we generated Na,K-ATPase constructs in which these residues are replaced by their H,K-ATPase counterparts either singly or in combinations. Surprisingly, none of the point mutants nor even the triple mutant was able to hydrolyze ATP at pH 6.0 at a rate greater than 20% of their respective V_{max}s. For the point mutants *L319F* and *N326Y*, protons seem to competitively inhibit ATP hydrolysis at pH 6.0, based on the low apparent affinity for Na^+ ions at pH 6.0 compared to pH 7.5. It would appear, therefore, that the cation selectivity of Na,K- and H,K-ATPase is generated through a cooperative effort between residues of transmembrane segments and the flanking loops that connect these transmembrane domains. This view is further supported by homology modeling of the Na,K-ATPase based on the crystal structure of the SERCA pump.

The Na,K- and gastric H,K-ATPases are members of the P-type class of ion-motive ATPases, a protein family that also includes the Ca-ATPases and yeast plasma membrane H-ATPase [for review, see (*1*)]. The characteristic feature of the members of this protein family is their ability to utilize the energy liberated through ATP hydrolysis to drive the transmembrane transport of cations against their electrochemical gradients. A great deal has been learned about the biochemical features of several P-type ATPases, including details of their substrate requirements, their reaction kinetics, and the relationship between these characteristics and the different conformational states of these enzymes (*2*−*5*). The recent publication of the 2.6 Å resolution crystal structure of the calcium pump of sarcoplasmic reticulum, which shares about 30% and 27% overall sequence identity with the α_1-Na,K-ATPase and the gastric H,K-ATPase, respectively, represents a major step forward in understanding structural features of P-type ATPases (*6*). However, presently very little is known about how the molecular and structural characteristics of the P-type pump proteins determine their individual functional properties.

The Na,K- and gastric H,K-ATPases are the two most closely related members of the P-type ATPase protein family. They both form functional heterodimers consisting of a larger α-subunit (∼110 kDa) and a highly glycosylated β-subunit (∼35 kDa core molecular mass) (*1*). The α-subunits of both enzymes probably incorporate all of the structural features required for enzymatic activity, whereas the β-subunits are necessary to ensure both the structural integrity of the dimeric protein complex as well as its proper delivery to the plasma membrane (*7*, *8*). Despite the fact that their α-subunits share 62% sequence identity, the two enzymes exhibit major functional differences. The Na,K-ATPase extrudes three Na^+ ions from the cytoplasm to the extracellular space in exchange for two K^+ ions, resulting in an overall transport cycle that is electrogenic. In contrast, the gastric H,K-ATPase has an electroneutral exchange stoichiometry. It is thought to secrete two protons in exchange for two potassium ions (*9*, *10*). The combination of their extensive similarity and their distinct functional repertoires suggests that these two enzymes might constitute an experimental system well suited to the investigation of the structural determinants responsible for their individual functional characteristics.

Our efforts to understand the structural features responsible for the unique activities of these pumps began with the functional analysis of protein chimeras. We previously reported that the N-terminal halves of the α-subunits of the Na,K- and H,K-ATPases in part determine their distinct ion specificities (*11*). The N-terminal half of each α-subunit

† This work was supported by grants from the NIH (GM42136 and DK17433).

* To whom correspondence should be addressed. Tel: (203) 785-7316, Fax: (203) 785-4951, E-mail: Michael.Caplan@yale.edu.

‡ Yale University School of Medicine.

§ McGill University.

10.1021/bi025819z CCC: $22.00
Published on Web 07/11/2002

includes the first four transmembrane domains (TM1−TM4)[1] as well as half of the large cytoplasmic loop connecting TM4 and TM5. A further dissection of this N-terminal half resulted in a chimera (*H85N/H309-519N*) in which only the TM3−TM4 ectodomain, TM4, and the N-terminal half of the TM4−TM5 cytoplasmic loop of the Na,K-ATPase α-subunit were replaced with their H,K-counterparts. When this chimera was expressed in LLC-PK_1 cells, it was observed to endow the host cells with the ability to acidify the surrounding extracellular medium (*12*). The examination of chimeras in which yet smaller segments of the Na,K-ATPase are replaced with the corresponding sequence from the H,K-ATPase demonstrated that the N-terminal half of the TM4−TM5 loop contributes to this effect. A chimera (*H85N/H356-519N*) composed of Na,K-ATPase sequence in which only this portion of the TM4−TM5 cytoplasmic loop derives from the corresponding region of the H,K-ATPase was able to hydrolyze ATP at pH 6.0 at more than 20% of its V_{max} in a Na^+-independent fashion. Little, if any, Na^+-independent ATPase activity is detected with the Na,K-ATPase wild-type enzyme, consistent with previous studies (*13*, *14*). These observations suggest that this chimera can exploit protons in place of sodium ions to support its catalytic cycle (*11*).

We next investigated the contribution of the TM3−TM4 ectodomain and residues of the fourth transmembrane segment TM4 to the determination of the distinct cation selectivities of the Na,K- and H,K-ATPases. A chimera in which the complete ectodomain and TM4 of Na,K-ATPase were substituted by its corresponding sequence from H,K-ATPase did not demonstrate measurable enzymatic activity. To circumvent this problem, we based subsequent pump constructs upon a helical wheel analysis of the TM4s of the Na,K- and H,K-ATPases.

The cation translocation pore of the Na,K- and H,K-ATPases, a structural domain that is likely to participate in the cation selection mechanism, is believed to be formed by TM4, TM5, and TM6 of the α-subunits (*15*). The SERCA crystal structure (*6*) further suggests that TM8 may also contribute to the translocation pore or the coordination of the cations during their translocation. Helical wheel analysis performed prior to the publication of the SERCA crystal structure suggested that three of the eight amino acid residues in TM4 that differ between the Na,K- and H,K-ATPase might face the presumed cation translocation pore. Therefore, they were considered as candidates that might contribute to the distinct cation specificities of these two pumps. We tested this hypothesis by creating the construct *ecto*+*A*, which incorporates the TM3−TM4 ectodomain from H,K-ATPase (resulting in mutations W312F and E314R) and substitutions of those three TM4 residues with their H,K-ATPase counterparts (L319F, N326Y, and T340S) into the background of the Na,K-ATPase α-subunit. Functional analysis revealed that at pH 6.0 this construct is able to hydrolyze ATP at more than 50% of its V_{max} in the absence of sodium ions, a property not observed for either native Na,K-ATPase pump or a control construct in which only the TM3−TM4 ectodomain is exchanged (*ecto*). Furthermore, we noted a 5-fold increase of the apparent Na^+ affinity at pH 6.0 compared to pH 7.5, which is kinetically consistent with the replacement of one or more Na^+ ions by protons in the pump transport cycle. These data, along with an observed strong pH-dependence of the Na^+-independent ATPase activity, supported the conclusion that protons can effectively drive the ATP hydrolysis mediated by the *ecto*+*A* chimera (*15*). (The kinetic data from this previous study are summarized in Table 1.)

Taken together, our results suggested that the three residues identified in TM4 are important in determining the cation selectivities of the pumps and the rates at which they undergo the conformational transitions characteristic of catalysis. In this study, we have examined the individual roles of these three residues in TM4. Surprisingly, the data demonstrate that none of the Na,K-ATPase mutants carrying only one of the three H,K-ATPase TM4 substitutions, nor a construct with two of those substitutions, and not even one with all three, was able to reproduce the functional characteristics of construct *ecto*+*A*. Comparison of the properties of the triple mutant with the *ecto*+*A* construct strongly suggests, therefore, that the TM3−TM4 ectodomain plays an unanticipated, critically important role in establishing the distinct cation selectivities of the Na,K- and H,K-ATPases.

EXPERIMENTAL PROCEDURES

Construction and Expression of Mutants. (A) Point Mutants. The mutants presented in this paper were constructed within the rat Na,K-ATPase α_1-subunit (cDNA provided by E. Benz, Johns Hopkins University). Starting material for the preparation of the point mutant constructs was a pBluescript vector containing the cDNA of the *H85N* construct, in which the *Acc*I and *Hpa*I sites had been silently introduced (*12*). In the first step, the cDNA was cut with *Acc*I and *Hpa*I, and the synthetic oligonucleotide 5′-ATAC-CTGGCT CGAGGCTGTC ATCTTCCTCA TTGGTAT-CAT CGTCGCGAAC GTGCCGGAAG GTTTGCTAGC CACCGTCACG GTATGTCTGA CGTT-3′ annealed to its complement 3′-TGGACCGAGC TCCGACAGTA GAAG-GAGTAA CCATAGTAGC AGCGCTTGCA CGGCCT-TCCA AACGATCGGT GGCAGTGCCA TACAGACTGC AA-5′ was ligated into the vector at these sites. This resulted in the silent introduction of restriction sites for *Nru*I at amino acid 325 and for *Nhe*I at amino acid 332 (amino acid numbers refer to the Na,K-ATPase sequence). After it was subjected to verification by sequencing through the ligation points, this new cDNA was then digested with either *Acc*I and *Nru*I, *Nru*I and *Nhe*I, or *Nhe*I and *Hpa*I. Annealed synthetic oligonucleotide inserts were ligated in to replace the original pump sequence between these sites. The fragment cut out with *Acc*I and *Nru*I was replaced by the oligonucleotide 5′-ATACCTGGCT CGAGGCTGTC ATCTTCTTCA TTGGTATCAT CGTCG-3′ and its complement 3′-TGGAC-CGAGC TCCGACAGTA GAAGAAGTAA CCATAG-TAGC AGC-5′, resulting in the mutation of a leucine to a phenylalanine at amino acid 319 (*L319F*). The fragment cut out with *Nru*I and *Nhe*I was replaced by the oligonucleotide 5′-CATATGTGCC GGAAGGTTTG-3′ and its complement 3′-GTATACACGG CCTTCCAAAC GATC-5′, which resulted in the mutation of amino acid 326 from an asparagine to a tyrosine (*N326Y*). It should be pointed out that this replacement did not reconstitute the *Nru*I site but rather led to the introduction of a *Nde*I site. Finally, the fragment cut out with *Nhe*I and *Hpa*I was replaced with the oligonucle-

[1] Abbreviations: TM, transmembrane domain; NMDG, *N*-methyl-D-glucamine.

otide 5′-CTAGCCACCG TCACGGTATG TCTGTCGTT-3′ and its complement 3′-GGTGGCAGTG CCATACAGAC AGCAA-5′, yielding the mutation of a threonine to a serine at amino acid 340 (*T340S*). All these digestions and ligations were performed in the pBluescript vector.

(B) Double and Triple Mutants. To obtain the double mutants L319F/N326F (*LFNY*) and L319F/T340S (*LFTS*), the cDNA of the construct *L319F* was used as starting material. To generate the double mutation construct *LFNY*, the cDNA was digested with *Nru*I and *Nhe*I, and the appropriate oligonucleotide designed for the single point mutations above was inserted by ligation. For the construction of *LFTS*, the cDNA was opened with *Nhe*I and *Hpa*I, and the matching oligonucleotide from above was ligated into the sites. Finally, cDNA of *LFTS* was digested with *Nru*I and *Nhe*I, and the oligonucleotide matching these sites (see above) was used to replace the excised fragment, thus producing the triple mutant L319F/N326F/T340S (*all*). The *LFTS* mutant was generated only for the production of *all*, and characterization of its enzymatic properties was not performed.

All mutants were stably expressed in LLC-PK_1 cells. For this purpose, the mutant cDNAs were subcloned behind a CMV promoter in the mammalian expression vector pCB6 (kindly provided by M. Roth, University of Texas Southwestern) which carries resistance to the antibiotic G418 (Gibco-BRL). The generation of the stable cell lines including transfection, antibiotic selection, screening for expression, and ouabain selection was carried out as described in (*12*).

Preparation of Membranes. The procedure to prepare membranes from the stably transfected LLC-PK_1 cells was performed as previously reported (*15*) with the following modification: In the earlier experiments, the protein yield of each preparation was determined with the BioRad protein assay. Since the protein concentration proved not to be a very useful predictor of activity, it was not performed for the preparations in this study. Instead, all of the membranes prepared from cells expressing the same mutant were pooled to ensure the greatest possible homogeneity of the membrane preparation. Subsequently, a small aliquot of the membrane suspension was tested for its ATPase activity. Appropriately sized aliquots of the membranes were then prepared so that each aliquot would yield the desired amount of activity in the ATPase assays. The aliquots were stored frozen at −80 °C

ATPase Assay. The ATPase assay used throughout this study was the same as previously reported (*15*−*17*). Each assay tube received 5−12 μg of the membrane preparations described above. Individual experiments were carried out in triplicate. The results were averaged and normalized to the maximal enzymatic activity (V_{max}), which was computed by fitting a Hill-function, $V = V_0 + V_{max}/\{1 + (K_{1/2}(X^+)/[X^+])^n\}$, to the data. Unless otherwise indicated, each individual experiment was performed at least 3 times. The data from the individual experiments were averaged, and again a Hill-function was fitted to the data. The values shown are the means of at least three experiments, and the error bars correspond to the standard deviation between the values obtained in individual experiments. The data are presented as the percentage of maximal activity (V_{max}). The values of the apparent $K_{1/2}$'s were also obtained from the same data fits.

To facilitate comparisons among the different mutant constructs, all ATPase assay data are normalized. However, to ensure the uniformity of reaction conditions, membranes were added to each test tube such that after a 2 h incubation period at 37 °C the colorimetric assay would yield an OD of 0.6−1.2, which corresponds to a concentration of about 150−300 μM free P_i in the 500 μL reaction volume, based on calibration curves. At pH 7.5, 75−80% of this signal could be suppressed in the presence of the high 5 mM ouabain concentration compared to the low 10 μM ouabain condition. At pH 6.0, the signal was reduced by 50−66% when the ouabain concentration was high. The assay was linear with time over its full 2 h course (data not shown).

SDS−PAGE and Western Blot Quantification. The membranes from cell lines expressing different mutants were diluted such that the samples were normalized for acitivity per sample volume. Samples were run on three 4−12% Tris−glycine Novex gradient gels (Invitrogen, Carlsbad, CA). The gels were run according to standard SDS−PAGE protocols. The protein was transferred to a PVDF membrane by semi-dry transblot (BioRad, Hercules, CA). The membrane was blocked with a 5% milk in TBS−Tween solution. The proteins were detected with the HK9 antibody that recognizes an epitope within the first 85 amino acids of the H,K-ATPase at a 1:1000 dilution. The secondary antibody, a goat anti-rabbit HRP-conjugated antibody from Sigma (St. Louis, MO), was used in a 1:60 000 dilution. Visualization of the bands was performed with the Enhanced ChemiLuminescence Plus kit from Amersham Biosciences (Piscataway, NJ).

Four different exposures of each gel were scanned in a 16-bit gray scale resolution on a flat-bed scanner (Microtek, Hsinchu, Taiwan). Subsequently, the signal intensity for each individual lane was measured with the MetaMorph software (Universal Imaging Corp., Downingtown, PA). The values for each individually scanned gel image were normalized to the intensity of the 10 μL sample of the *H85N* membranes; the values from the four different exposures of the same gel were averaged after the normalization. Finally, the intensity values for the three different gels were averaged and plotted. The error bars reflect the standard deviation among the normalized, averaged intensity values for the three separate gels (Figure 2B).

Structure Modeling. The availability of the crystal structure coordinates of the SERCA pump (*6*) allowed us to perform structure comparison and homology modeling. The CLUSTAL program (*18*) was used for initial sequence alignment, and the SwissPDBViewer software and the ProModII software run on the SWISS-MODEL server (*19*, *20*) were used to generate a structural model of the Na,K-ATPase based on the SERCA ATPase structure. The overall sequence identity between the SERCA pump and the sodium pump is almost 28%, and the sequence similarity between the two pumps is about 45%. This degree of identity and similarity is high enough to justify the assumption that these proteins exhibit the same general protein folding patterns. This view is supported by recent electron density data from Rice and co-workers (*21*). Their 11 Å electron density map of the Na,K-ATPase is in very good agreement with the electron density map of the SERCA pump. Noticeable differences between the two electron density maps correlate very well with insertions or gaps in the primary sequence alignment. The sequence identity within the transmembrane domains

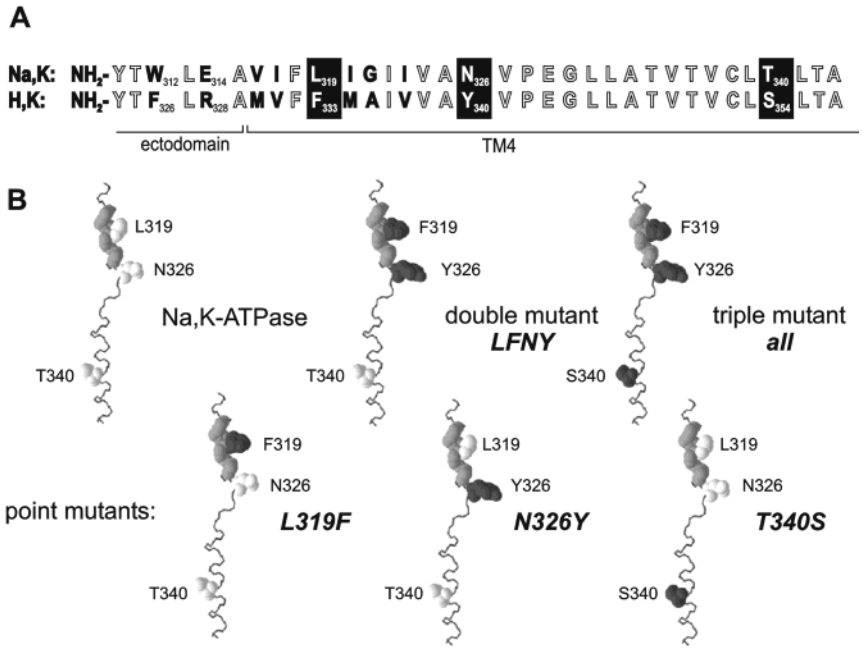

FIGURE 1: Helix representations of the TM4 mutants employed in this study. (A) Of the 29 amino acids which are thought to form TM4, only 8 differ between Na,K- and H,K-ATPase. They are depicted in black boldface. Also shown is the sequence of the TM3−TM4 ectodomain that is changed from the Na,K-ATPase sequence to the H,K-ATPase sequence in the chimeras *ecto* and *ecto*+*A*. (B) Helix depictions of the native TM4 from the Na,K-ATPase α-subunit and of the TM4s of all constructs used in this study. The depiction of the TM4 helix is derived from modeling of the Na,K-ATPase, based upon the solved structure of the Ca-ATPase (*6*) (see Figure 7). In the wild-type Na,K-ATPase TM4, the backbone atoms of amino acids that differ between the two pumps are shown in gray spacefill. The residues which were mutated in this study are depicted, along with their side chains, in white spacefill. In the TM4s of the mutant constructs, dark gray marks the substitution of the Na,K-ATPase residues with their H,K-ATPase counterparts. All of the TM4 mutation constructs were generated in the context of *H85N* (*11*).

is significantly higher than the overall identity. With respect to the pore-forming TM4, TM5, and TM6 helices, which share 39% identity and 71% similarity, therefore, our model probably represents the real Na,K-ATPase structure to a reasonably good approximation. Based on the 3DCrunch Project (see http://www.expasy.ch/swissmod/SWISS-MODEL.html), 63% of models for which the target shares 40−49% sequence identity with the template are correct with a root-mean-square difference value lower than 3 Å.

RESULTS

We have previously shown that residues Leu[319], Asn[326], and Thr[340] of the Na,K-ATPase, and their counterparts Phe[333], Tyr[340], and Ser[354] of the gastric H,K-ATPase, may potentially contribute to establishing these pumps' distinct cation selectivities (*15*). In this study, the functional contributions of these residues were examined in the context of a Na,K-ATPase α-subunit construct in which these three residues, as well as the sequence of the ectodomain connecting transmembrane segments 3 and 4, derive from the comparable regions of the gastric H,K-ATPase α-subunit (*ecto*+*A*). To examine further whether and how the properties of *ecto*+*A* are conferred by these substitutions, we analyzed Na,K-ATPase mutant constructs which have one or several of the relevant transmembrane residues replaced with their H,K-ATPase counterparts. The designs of the constructs tested are presented in Figure 1. The constructs were analyzed through ATPase activity assays performed on crude plasma membrane fractions prepared from stably transfected LLC-PK$_1$ cells.

Assessment of Total Turnover Numbers. Prior to examining the apparent cation affinities of our constructs, we wished to establish that they manifest similar levels of intrinsic enzymatic activity. We selected five key constructs, therefore, and assayed their relative turnover numbers by determining the quantity of pump protein necessary to liberate the same amount of inorganic phosphate from ATP per unit time under V_{max} conditions (100 mM Na^+, 20 mM K^+, 3 mM ATP, pH 7.5). Only the ouabain-sensitive fraction of the inorganic phosphate release was considered for this normalization. The quantification of three independent Western blots in Figure 2B shows that the amount of enzyme needed to achieve the same ouabain-sensitive ATP consumption does not vary significantly among the control construct *H85N* and the mutant constructs *ecto*, *ecto*+*A*, *LFNY*, and *all*. Thus, the overall turnover number for each of the mutant constructs appears not to be significantly altered compared to the wild-type enzyme.

Na^+-Dependence of ATPase Activity. As previously reported (*15*), we have observed a dramatic 5-fold increase in the apparent Na^+-affinity of construct *ecto*+*A* at pH 6 compared to pH 7.5 (Figure 3F). We used the same experimental conditions to assess the Na^+-dependence of the ATPase activity of all of the new mutant constructs both at pH 7.5 and at pH 6. At pH 7.5, the observed $K_{1/2}$ values all correspond well to our earlier findings for *H85N*, *ecto*, and *ecto*+*A* (see Table 1). As for those constructs, the $K_{1/2}(Na^+)$s of the point mutants did not differ very much from the values that have been reported for the wild-type sodium pump [$K_{1/2}$ = 7.1 mM under similar conditions, (*22*)], except for *N326Y*, which displayed a ∼1.5-fold elevation in $K_{1/2}(Na^+)$. The $K_{1/2}(Na^+)$ values are listed in Table 1, and the data are shown in Figure 3A−C.

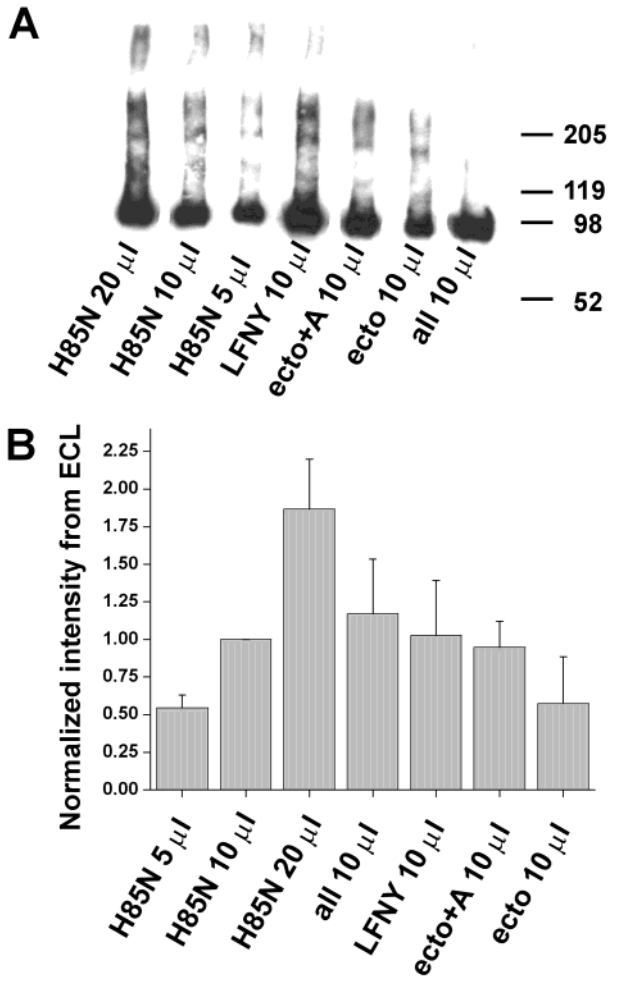

FIGURE 2: Quantification of Western blots of mutant constructs. (A) This figure shows one of the three Western blots used to quantitate the signal intensity of membranes from LLC-PK_1 cells which stably express the wild-type-like control *H85N* or the mutant constructs *LFNY*, *ecto*+*A*, *ecto*, or *all*. The samples loaded are membranes which were diluted in such a way that in ATPase assays for each construct the same volume of membrane suspension would yield the same amount of ATP hydrolysis. (B) This plot illustrates the quantification of Western blot signal intensities of several key pump constructs used in this and the previous study (*15*). The signal intensities from three separate Western blots were averaged and normalized to qualitatively compare the turnover numbers of the constructs *H85N*, *all*, *LFNY*, *ecto*, and *ecto*+*A*. It was found that the chemiluminscence intensity for 10 μL of membranes was very similar for all five constructs. Error bars represent the standard deviation among the three separate Western blots. This demonstrates that the total turnover rates of the various mutant constructs are not substantially different from each other and from the wild-type-like control *H85N* (for technical details, see Experimental Procedures).

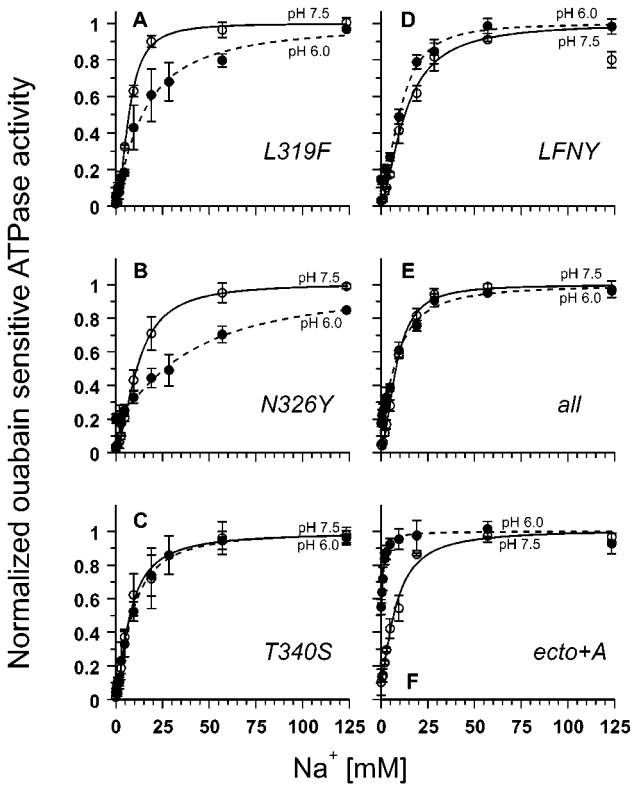

FIGURE 3: Na-dependence of ouabain-sensitive ATPase activity. Na titrations of the ATP hydrolysis activity were carried out at pH 7.5 (○) and pH 6.0 (●). The incubation solution contained 3 mM ATP, 3 mM Mg^{2+}, and 20 mM K^+. The endogenous Na,K-ATPase was inhibited by addition of 10 μM ouabain. For comparison, panel F shows the data previously obtained for *ecto*+*A*. Clearly, none of the TM4 mutations, including the triple mutant *all*, comes close to reproducing the sodium dependence behavior observed for the *ecto*+*A* construct.

In marked contrast to our observations with construct *ecto*+*A*, none of the three point mutants showed an increase in the apparent Na^+-affinity at pH 6.0 as compared to that measured at pH 7.5. Instead, for both *L319F* and *N326Y*, we observed a striking reduction in the apparent Na^+ affinity at pH 6 compared to pH 7.5, i.e., 2-fold for *L319F* and 3.5-fold for *N326Y* (Table 1 and Figure 3A,B). The mutant *T340S* did not behave differently from our wild-type control *H85N* (Figure 3C). None of the mutants were capable of hydrolyzing ATP at pH 6.0 in a Na^+-independent fashion as effectively as construct *ecto*+*A* (53%) (Figure 3F). Nevertheless, as discussed further below, *N326Y* showed a Na^+-independent ATPase activity of about 20% of its V_{max}.

Since none of the single point mutants reproduced the functional characteristics of *ecto*+*A*, we investigated the Na^+-dependence of the ATPase activities of the double mutant *LFNY* and the triple mutant *all*, again at pH 7.5 and at pH 6 (Figure 3D,E). At pH 7.5, the $K_{1/2}(Na^+)$ for *all* was essentially unchanged compared to the wild-type-like *H85N* and to *ecto*+*A*. The apparent Na^+-affinity of *LFNY* was similar to that of *N326Y*, being ~50% reduced. It should be pointed out that the constructs *all* and *LFNY* differ only in the T340S substitution, which by itself did not yield any effect on the apparent Na^+-affinity.

At pH 6, both *LFNY* and *all* exhibited pH-dependent changes in apparent affinities which are subtle (Table 1 and Figure 3D,E), albeit statistically significant based on the Student's *t*-test ($p < 0.01$ for *all* and $p < 0.05$ for *LFNY*). Furthermore, both constructs displayed only small Na^+-independent ATPase activities at pH 6.0 (21% and 14% for *all* and *LFNY*, respectively). Thus, these two constructs clearly do not possess functional properties that emulate those observed for the construct *ecto*+*A* (Figure 3F). The fact that *ecto*+*A* and *all* differ only in the origins of their TM3−TM4 ectodomains presents surprising evidence in support of an extremely important role for an ectodomain pump segment in enabling the chimeric constructs to utilize protons instead of Na^+ ions to drive the hydrolysis of ATP.

Table 1: Summary of Kinetic Data[a]

	Na^+-dependence $K_{1/2}(Na^+)$ (mM)		Na^+-independent activity (%)	K^+-dependence $K_{1/2}(K^+)$ (mM)		vanadate inhibition IC_{50} (μM)	activity at 2.5 mM vanadate (%)
	pH 7.5	pH 6.0	pH 6.0	pH 7.5	pH 6.0	pH 7.5	pH 7.5
L319F	7.1 ± 0.3	15.4 ± 2.35	7	3.0 ± 0.17	2.5 ± 0.17	162 ± 23	34
N326Y	11.7 ± 0.21	38.6 ± 9.1	20	1.44 ± 0.13	2.1 ± 0.22	176 ± 26	31
T340S	7.3 ± 0.9	9.2 ± 0.6	6	1.27 ± 0.11	0.78 ± 0.1	39 ± 6	0
LFNY	13.2 ± 1.2	11.5 ± 0.6	14	3.1 ± 0.34	7.5 ± 2.6	97 ± 45	51
all	8.4 ± 0.32	9.6 ± 0.9	21	2.5 ± 0.18	2.6 ± 0.27	80 ± 53	57
H85N[b]	8.4 ± 0.7	9.2 ± 0.3	7	1.2 ± 0.1	0.74 ± 0.1	14.9 ± 2.4	9
ecto[b]	9.5 ± 0.6	5.6 ± 0.7	13	2.8 ± 0.15	1.4 ± 0.2	41.6 ± 9.9	25
ecto+A[b]	8.2 ± 1.0	1.5 ± 0.1	53	4.6 ± 0.5	2.5 ± 0.4	151.0 ± 41.3	58

[a] Summary of all $K_{1/2}$ and IC_{50} values determined in this study and comparison to constants from a previous study. All values are given in millimolar, except for vanadate IC_{50}, in which is given in micromolar. All ATPase activity experiments were performed in the presence of 3 mM ATP, 3 mM Mg^{2+}, and 10 μM ouabain to inhibit endogenous Na,K-ATPase. Sodium titrations were performed in the presence of 20 mM K^+, potassium titrations in the presence of 100 mM Na^+, and vanadate titrations in the presence of 20 mM K^+ and 100 mM Na^+. Constant ionic strength was ensured by adding appropriate concentrations of NMDG. In the fourth column, the Na^+-independent ATPase activity at pH 6.0 is given in percent of V_{max} at pH 6.0. The last column displays the remaining ATPase activity in the presence of nominally about 2.5 mM othovanadate. [b] From previous study (*15*).

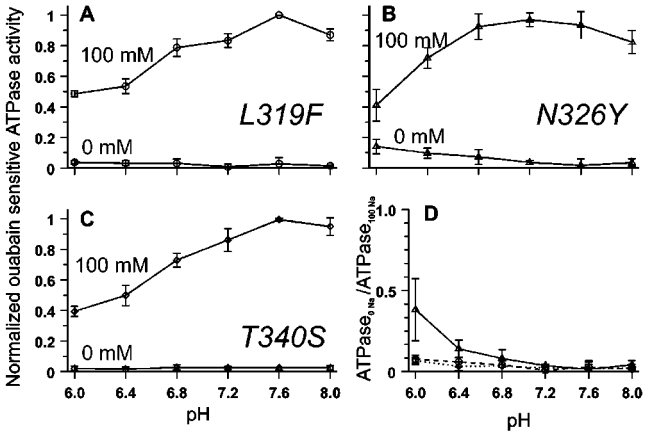

FIGURE 4: pH-dependence of sodium-independent ouabain-sensitive ATP hydrolysis. The pH-dependence of the ATPase activity was determined with 100 and 0 mM Na^+ in the incubation solution. The solutions also contained 3 mM ATP, 3 mM Mg^{2+}, 20 mM K^+, and 10 μM ouabain to abolish the endogenous sodium pump activity. At 100 mM Na^+, the pH-dependence of the ATPase activity for *L319F* (A) and *T340S* (C) is almost identical to what has been observed for wild-type Na,K-ATPase. In contrast, the mutant *N326Y* (B) appears to have its pH optimum slightly shifted from pH 7.6 down to pH 7.2. (D) The plot represents the fraction of sodium-independent ATPase activity detected at different pH-values. A measurable pH-dependent Na^+-independent activity can be seen only for mutant *N326Y*.

pH-Dependence of ATPase Activity. To gain further insight into whether protons drive the Na^+-independent ATPase activity observed for *N326Y*, we examined the pH-dependence of the Na^+-independent ATP hydrolysis catalyzed by this mutant. An increase in the magnitude of the Na^+-independent ATPase with decreasing pH-values would be expected if, indeed, protons were substituting for Na^+ ions. The experiments are summarized in Figure 4. The graphs for the individual mutants show that *L319F* (Figure 4A) and T340S (Figure 4C) do not differ from the behavior observed for the wild-type-like control H85N (*15*). With a concentration of 100 mM Na^+ present in the incubation solution, they achieve their pH-dependent activity maximum around pH 7.6. In the absence of Na^+, no significant ATPase activity can be observed. In contrast, for *N326Y* the pH-dependence of the ATPase activity maximum is slightly shifted from pH 7.6 (Figure 4A,C) to approximately pH 7.2 (Figure 4B). Furthermore, *N326Y* is the only construct for which a small Na^+-independent, pH-dependent ATP hydrolysis activity (defined as the ratio of ATPase activity at 0 mM Na^+ to that measured at 100 mM Na^+) is detected (Figure 4D). The pH-dependence is similar to that previously seen for *ecto+A*. An increase in pH of 0.4 pH unit, corresponding to a 2.5-fold decrease in proton concentration, results in approximately a 50% decrease of Na-independent enzyme activity. These findings support the hypothesis that at least Asn^{326} of the sodium pump and its counterpart, Tyr^{340} of the H,K-ATPase, are involved in establishing the specificity of these enzymes for either Na^+ ions or protons.

K^+-Dependence of ATPase Activity. Our data establish clearly that the TM4 mutants are unable to reproduce the Na^+- and pH-dependencies observed for the construct *ecto+A*. We then measured the K^+-dependence of the ATPase activity for all of the mutant constructs to further compare them to *ecto+A* (Figure 5). In identical measurements, *ecto+A* had shown a 4-fold reduced apparent K^+-affinity compared to the wild-type-like *H85N* (Table 1). We found that the behavior of the point mutation constructs with respect to K^+ ions was surprisingly complex. The determined $K_{1/2}(K^+)$ values are listed in Table 1. At pH 7.5, all constructs, with the exception of *T340S*, had a lower apparent K^+-affinity than *H85N*. However, none of the reductions were as dramatic as that observed for *ecto+A* (Figure 5F). Only the mutant *T340S* exhibited the 2-fold decrease in $K_{1/2}(K^+)$ at pH 6.0 previously observed for *H85N*, *ecto*, and *ecto+A* (Table 1). The other constructs displayed changes ranging from mildly reduced to unchanged $K_{1/2}(K^+)$ values (*L319F* and *all*, respectively) to elevated or drastically elevated $K_{1/2}(K^+)$ values (*N326Y* and *LFNY*, respectively). It is evident from this complex pattern that none of the mutant constructs reproduce the K^+-dependence that was seen for *ecto+A*. Once again, the differences between the findings for the TM4 mutants and those obtained with *ecto+A* emphasize the importance of the TM3−TM4 ectodomain in determining properties of the cation binding sites in the Na,K- and gastric H,K-ATPase.

Interestingly, as was seen for the Na^+-dependence of the ATPase activity, the K^+-dependence data for *LFNY* and *all*

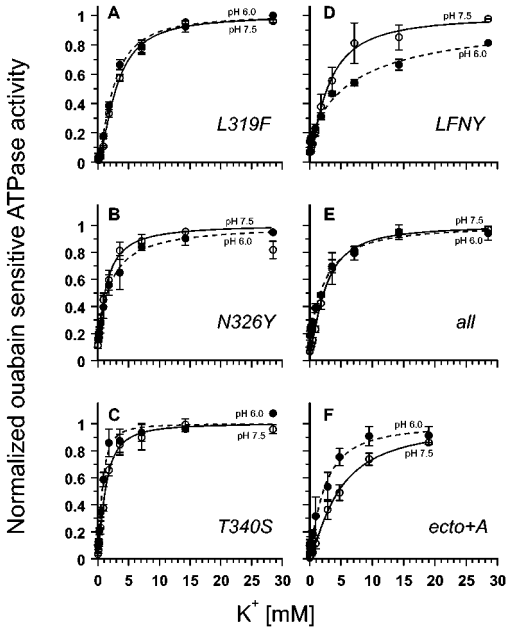

FIGURE 5: K-dependence of ouabain-sensitive ATPase activity. K-dependent ouabain-sensitive ATPase activity was measured at pH 7.5 (○) and pH 6.0 (●). The incubation solution contained 3 mM ATP, 3 mM Mg^{2+}, and 100 mM Na^+. To inhibit the endogenous sodium pump, all solutions contained 10 μM ouabain.

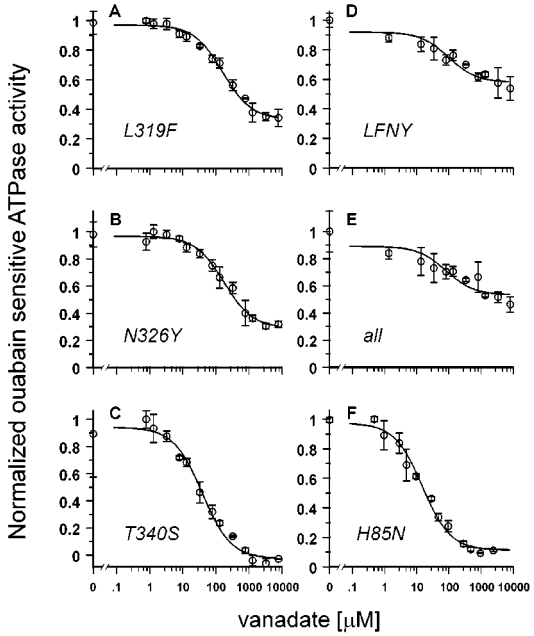

FIGURE 6: Vanadate inhibition titration of ouabain-sensitive ATPase activity. The ATPase assay was carried out with 3 mM ATP, 3 mM Mg^{2+}, 100 mM Na^+, and 20 mM K^+ in the incubation solution. The solution also contained 10 μM ouabain to suppress contributions from the endogenous sodium pump. Due to the limited solubility of orthovanadate, most mutants cannot be inhibited to the level that can be achieved by ouabain inhibition (zero-activity level). Thus, the activity remaining at the highest vanadate concentration is likely to provide a better indication of the magnitude of the vanadate IC_{50} shift than the actual computed IC_{50} values (Table 1). When compared to the inhibition of the wild-type-like *H85N* (F) [from (*15*)], the data illustrate that the mutants *L319F* (A), *N326Y* (B), *LFNY* (D), and *all* (E) have a lower sensitivity to vanadate, suggesting a shift in the conformational equilibrium of these constructs toward the E_1 conformations. In contrast, the sensitivity of *T340S* (C) does not appear to be affected. Based on the magnitude of the residual noninhibitable activity, the mutants *LFNY* and *all* seem to be even less sensitive to vanadate than the point mutants *L319F* and *N326Y*.

again show that the interchange of residues Thr^{340} of the Na,K-ATPase and Ser^{353} of the gastric H,K-ATPase produces functionally significant consequences only in the presence of additional residue replacements. The mutation T340S in the background of the Na,K-ATPase does not measurably change the properties of the wild-type pump, whereas it seems to exert a synergistic effect when combined with the other mutations.

Orthovanadate Sensitivity of ATPase Activity. In the previous study, we reported a dramatic shift in the orthovanadate sensitivity of construct *ecto+A* compared to the wild-type-like *H85N*. Orthovanadate ions act as analogues of inorganic phosphate ions and inhibit P-type ATPases. Like K^+, they bind in the E_2 conformation of the enzyme. The vanadate-IC_{50} of *ecto+A* was strongly reduced, consistent with an E_1/E_2 conformational equilibrium shift toward the E_1 conformation (*15*, *23*). This proposed change in conformational equilibrium correlated well with the reduced apparent K^+-affinity in this construct (see Table 1).

We measured the $IC_{50}(VO_4^{3-})$ values of all the mutant constructs to determine the contribution of the individual TM4 residues to the altered vanadate sensitivity of *ecto+A* and to the inferred shift in the E_1/E_2 conformational equilibrium. The data are shown in Figure 6 , and the $IC_{50}(VO_4^{3-})$ values, based on fits to a Hill-function with the Hill-coefficient fixed to 1, are listed in Table 1. The level of vanadate inhibition achieved for both *L319F* and *N326Y* (Figure 6A,B) was less than the inhibition obtained with 5 mM ouabain (corresponding to zero activity in the graphs). This discrepancy appears to be due to a limited solubility of orthovanadate in our assay solutions. Therefore, vanadate IC_{50} values for mutants that were not fully inhibited by vanadate are likely only lower estimates of the real inhibition constants. Nevertheless, the determined $IC_{50}(VO_4^{3-})$ values are consistent with the interpretation that both *L319F* and *N326Y* have conformational equilibria that are shifted toward the E_1 states compared to the wild-type sodium pump. The mutant *T340S*, which did not show any appreciable difference from the wild-type enzyme in all other experiments, exhibited a modest 2.5-fold increased $IC_{50}(VO_4^{3-})$ compared to *H85N* (Figure 6C,F).

The double mutant *LFNY* and the triple mutant *all* exhibited inhibition characteristics that were almost identical to one another when these constructs were incubated with orthovanadate (Figure 6D,E). The computed apparent IC_{50} values are only moderately elevated (Table 1), but it must be noted that less than 50% of the ouabain-inhibitable activity could be inhibited with vanadate. This demonstrates once again that the apparent IC_{50} values are substantial underestimates. These inhibition characteristics of *LFNY* and *all* are paralleled by that of the *ecto+A* construct, for which only 40% of the ouabain-sensitive activity could be inhibited with orthovanadate. It appears, therefore, that the level of vanadate inhibition compared to the ouabain inhibition level might represent a sensitive indicator for the magnitude of a conformational equilibrium shift (the corresponding numbers are included in Table 1). Thus, the constructs that experience the least inhibition by orthovanadate compared to the level of ouabain inhibition are characterized by the most significant E_1/E_2 equilibrium shifts toward the E_1 conformations. Ac-

cording to this interpretation, both *LFNY* and *all* experience large conformational equilibrium shifts compared to the wild-type-like *H85N*.

DISCUSSION

Our previous work had suggested that residues Leu^{319}, Asn^{326}, and Thr^{340} of the Na,K-ATPase and their counterparts Phe^{333}, Tyr^{340}, and Ser^{354} of the gastric H,K-ATPase play critical roles in the cation selectivities of these two P-type ATPases (*15*). The aim of this study was to elucidate the roles of these TM4 residues in distinguishing between Na^+ ions and protons and to explore the importance, if any, of the TM3−TM4 ectodomain for the distinct cation selectivity of the Na,K- and H,K-ATPases.

Our original interest in these three TM4 residues was based on a helical wheel analysis suggesting that they constitute the only TM4 residues that differ among the Na,K- and H,K-ATPases which might be expected to line the cation translocation pore. We used modeling to perform a comparison of the cation translocation pores in the E_1 conformations of the SERCA pump (from the crystal structure) and the Na,K-ATPase (based on homology modeling). It appears that of the eight residues that differ between the two pumps, the side chains of two of the amino acids that we initially identified in our helical wheel analysis are the most appropriately positioned to participate in cation coordination (Leu^{319} and Asn^{326} of the Na,K-ATPase and their counterparts Phe^{333} and Tyr^{340} of the gastric H,K-ATPase). All other side chains that differ between the Na,K- and H,K-ATPase are predicted to point away from the presumed pore (Figure 7). It must be noted that backbone carbonyl groups are also capable of conferring cation specificity. For both the SERCA pump and the KcsA potassium channel, it has been shown that backbone carbonyl groups play important roles in the coordination of translocated cations (*6*, *24*). This fact had previously been established for the gramicidin channel (*25*, *26*). Comparison of our models of the Na,K-ATPase with models of *ecto* and *ecto*+*A* chimeras shows slight alterations in the backbone of TM4 upstream of Leu^{319} or Phe^{319}, respectively, indicating that the positions of backbone carbonyls might be changed in the mutated constructs. However, the side chain of the third amino acid that we identified in the helical wheel analysis, Thr^{340} of the sodium pump and its counterpart Ser^{354} of the H,K-ATPase, does not seem to line the pore in the model of the E_1 conformation. The SERCA crystal structure shows an unwound section in the TM4 helix from amino acid 307 to 310 of the SERCA sequence. Because of its location downstream from this helix break in TM4, our original prediction of the position of Thr^{340} and Ser^{354} based on a helical wheel model was not correct.

To gain further insight into the roles of these three TM4 residues, which we had previously mutated in the *ecto*+*A* construct, we analyzed the point mutant constructs *L319F*, *N326Y*, and *T340S* as well as the double mutant *LFNY* and the triple mutant *all*. We found that only TM4 mutants that incorporated the N326Y substitution were capable of generating any Na^+-independent activity. This activity never exceeded 20% of the respective V_{max}s. The pH-dependence of the Na^+-independent activity for *N326Y* (Figure 4D) was virtually the same as that of *ecto*+*A*, supporting the hypothesis that in some of our constructs (*N326Y*, *LFNY*, *all*, and *ecto*+*A*) protons can substitute for Na^+ ions to drive the ATP hydrolysis. Nevertheless, even the triple mutant *all* did not come close to reproducing the functional characteristics observed for *ecto*+*A*. None of the mutants that carried substitutions in TM4 in the absence of the ectodomain substitution showed a higher apparent Na^+-affinity at pH 6.0 compared to pH 7.5, as was observed for *ecto*+*A* and also for *ecto* (see Table 1). In fact, for the point mutants *L319F*

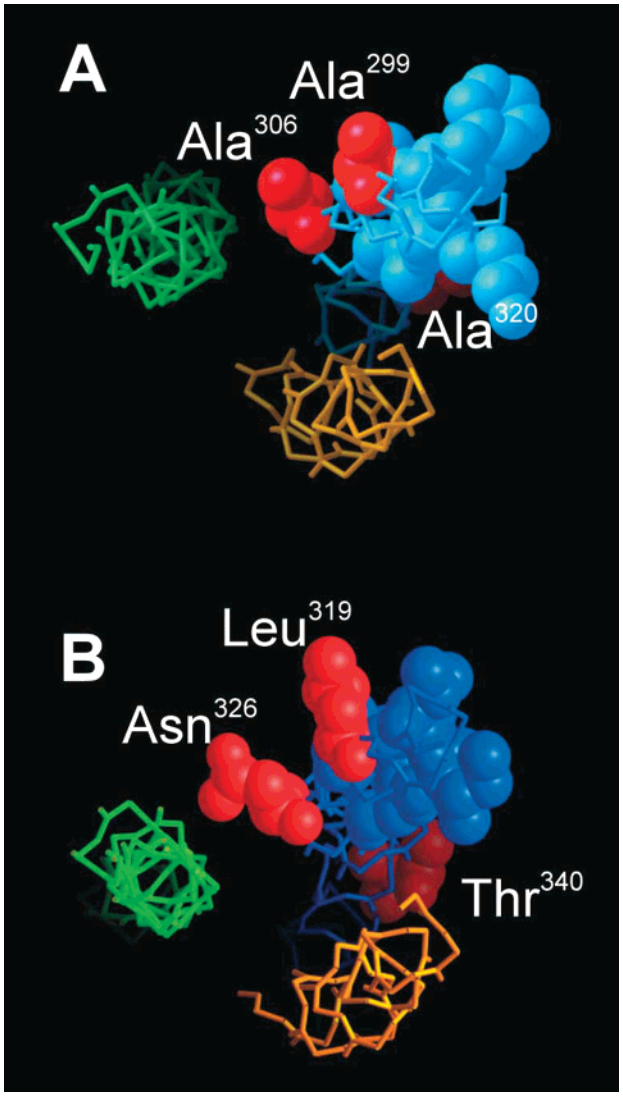

FIGURE 7: View into the cation translocation pores of SERCA and Na,K-ATPase from the extracellular side. Panel A shows the SERCA pore. The coordinates are taken directly from the published crystal structure. Panel B shows the pore of the Na,K-ATPase as part of the complete sodium pump structure model. For both the SERCA and the Na,K-ATPase, the TM4s are in blue, the TM5s are in green, and the TM6s are in yellow. Except for the amino acid residues depicted in the spacefill representation, only the backbone atoms have been included in this image. The amino acids shown in red spacefill are those which had been identified by helical wheel analysis to potentially confer cation specificity in the sodium pump through side chain interactions (B). The corresponding positions in the SERCA pump are also shown in red (A). The residues in blue spacefill are those which are different between Na,K- and H,K-ATPase but were thought not to influence cation selectivity because the helical wheel analysis predicted them to face away from the presumed pore. The crystal structure and the model confirm the prediction that the side chains of all amino acids in blue point away from the pore. In contrast to the prediction, however, residue Thr340, which is located downstream from the helix break in TM4, faces away from the pore.

and *N326Y*, the opposite was true. These two pump mutants displayed strongly reduced apparent Na^+-affinities at pH 6.0. These results suggest that at low pH protons can displace Na^+ ions from the binding sites of *L319F* and *N326Y*, but the interactions of those protons with the mutant pumps are ineffective in driving the catalytic cycle. Protons appear to be able to promote a small Na^+-independent ATPase activity; however, they appear primarily to compete with Na^+ ions for their binding sites or interact with the mutant constructs in such a way that Na^+ ions cannot properly interact with their binding sites. These two constructs appear to require substantially increased Na^+ concentrations (as compared to wild-type enzyme) in order to compete away the protons and effectively drive the catalytic turnover at pH 6.0. Thus, protons appear to act as weak competitive inhibitors of the Na,K-ATPase activity of these constructs.

The observations for the apparent Na^+ affinities allow only one explanation for the differences between the behavior of *ecto+A*, on the one hand, and that of the single, double, and triple mutants, on the other hand: the TM3−TM4 ectodomain must play a crucial role in establishing the distinct substrate specificity and kinetic properties of the two cation pumps. It would appear, therefore, that the substantial alterations in cation selectivity detected with *ecto+A* are not attributable to the TM4 or the ectodomain substitutions alone, but are the product of a cooperative interaction between TM4 and the adjacent TM3−TM4 ectodomain.

Recent observations suggest that the domain containing TM3, TM4, and the intervening ectodomain of the Na,K-ATPase is in part necessary to confer high ouabain sensitivity to chimeras generated from Na,K- and gastric H,K-ATPase (*27*). The same domain is also included in the stretch comprising TM1−TM6 of the Na,K-ATPase that is able to confer Na^+-dependence upon H,K/Na,K-ATPase chimeras (*28*). These findings are consistent with our conclusion that cooperative interactions between extracellular domains and transmembrane segments may significantly influence functional properties of P-type ATPases.

Our data indicate that the observed shifts in the apparent K^+-affinity correlate reasonably well with the measured shifts in the extent of vanadate sensitivity. These observations suggest that the introduced point mutations in TM4, either by themselves or in combinations of two or three, can produce shifts in conformational equilibria. We cannot, however, exclude the possibility that alterations to the intrinsic K^+-affinity may contribute directly to the changes in apparent K^+-affinity (*29*). Thus, for example, the possibility exists that in the constructs *LFNY* and *N326Y* the K^+ binding sites have been altered so that protons compete with potassium ions, resulting in lower apparent K^+-affinities at pH 6. This alternative receives support from the fact that both *N326Y* and *LFNY* show a significant K^+-independent ATPase activity. Similarly, a change in sensitivity to orthovanadate is not strictly indicative of a change in the E_1/E_2 conformational equilibrium. We cannot discriminate between a decrease in sensitivity to orthovanadate due to a conformational equilibrium shift toward the E_1 conformations or merely to a change in a rate-limiting step, i.e., the acceleration of the occlusion step following the loss of the inorganic phosphate.

It is somewhat surprising that despite the possible shifts in conformational equilibrium toward the E_1 states that we presume to affect many of the constructs examined in this study, most of the $K_{1/2}(Na^+)$ values do not decrease. One might expect that accumulation of enzyme in an E_1 state would result in an increased apparent affinity for Na^+. We postulate that this effect is not seen because it is masked by an increase in the intrinsic proton affinity of the Na^+ binding sites, which in turn lowers the apparent Na^+-affinity due to competitive proton binding to the Na^+ binding sites. At lower pH, there is even more competitive binding, consistent with the reduced apparent affinity for sodium ions that is seen for most constructs at pH 6 compared to pH 7.5. It is interesting to note that the association between alterations in TM4 and shifts toward E_1 conformations has been previously detected for other TM4 substitutions (*30*−*33*). This correlation strongly suggests that transitions between the E_1 and E_2 states involve substantial modifications in the structure of TM4 and the kinetics of the conformational transition are exquisitely sensitive to changes in the primary structure of TM4.

Our findings for *N326Y* are consistent with the results of a previous mutagenesis study designed to identify residues that might serve as cation ligands. In that case, the asparagine at position 326 of the Na,K-ATPase was replaced with a leucine residue (*22*). As a result of this mutation, the affinity for sodium ions decreased more than 3-fold to 24 mM, while the affinity for potassium ions did not seem to change significantly. Further experiments demonstrated that the decreased Na^+-affinity was not attributable to a shift in conformational equilibria toward the E_2 conformation. The possibility of a conformational equilibrium shift toward the E_1 states was not assessed in that study.

In addition to Asn^{326}, the residues Glu^{329}, Glu^{781}, and Thr^{809} have been classified as potential Na^+ ligands at the high-affinity cytoplasmic sites in the E_1 form of the sodium pump (*34*). Except for Asn^{326}, these residues are highly conserved among P-type ATPases, and they are identical between the Na,K- and gastric H,K-ATPase (*1*, *34*, *35*). This would suggest that at least some of the residues involved in cation binding are shared among different pumps and do not play a role in determining cation specificity. This consideration further supports the notion that Asn^{326} may indeed play a critical role in distinguishing between Na^+ ions and protons. Two different mechanisms can be imagined: (1) the cation coordination in the cation binding pocket is altered because the contributing side chain is different or (2) the altered side chain results in a modified backbone conformation such that backbone carbonyl groups involved in cation coordination are arranged differently. Unfortunately, the molecular modeling discussed above does not allow us to choose among these two possibilities. Since the conformational rotamer of the altered side chains can be varied when introducing a side chain substitution into a model, it is possible to create models that would support either of the two mechanisms equally well.

In conclusion, our findings suggest that the distinct cation specificities of the Na,K- and H,K-ATPases are achieved through complex interactions among several protein domains. Amino acids within the transmembrane domains clearly participate in cation binding, but it seems that these amino acids are not by themselves capable of establishing cation selectivity of ATPase activity. Residues on either side of the lipid bilayer must participate in the formation of

optimized binding sites, selective access pathways to those binding sites, and specific catalytic conformations. We have shown that the TM3−TM4 ectodomain, the three discrete residues within the TM4 helix, and the TM4−TM5 cytoplasmic loop are major determining factors in the differential cation selectivities exhibited by these pumps. The crystal structure of the SERCA pump and comparative protein structure modeling allow us to speculate on the mechanisms by which these pump domains interact to achieve specificity, but experimental proof for these mechanisms is not currently available.

This study, together with previous work form our laboratory and from other groups (*27*, *28*), demonstrates the critical importance of synergistic interactions of transmembrane segments and extracellular domains, as well as interactions of residues within these domains. Our findings underscore the complex and cooperative nature of cation translocation by P-type ATPases.

ACKNOWLEDGMENT

We are grateful to Tobene Anakwe for excellent technical support. We are indebted to Lisa Dunbar, Biff Forbush, Fred Sigworth, and Clifford Slayman for valuable discussions and advice. Finally, we thank Carolyn Slayman and David Gadsby for discussion and critique of the manuscript.

REFERENCES

1. Moller, J. V., Juul, B., and le Maire, M. (1996) *Biochim. Biophys. Acta 1286*, 1−51.
2. Bonting, S. L., de Pont, J. J., van Amelsvoort, J. M., and Schrijen, J. J. (1980) *Ann. N.Y. Acad. Sci. 341*, 335−356.
3. Heyse, S., Wuddel, I., Apell, H. J., and Sturmer, W. (1994) *J. Gen. Physiol. 104*, 197−240.
4. Rabon, E., Cuppoletti, J., Malinowska, D., Smolka, A., Helander, H. F., Mendlein, J., and Sachs, G. (1983) *J. Exp. Biol. 106*, 119−133.
5. Skou, J. C., and Esmann, M. (1992) *J. Bioenerg. Biomembr. 24*, 249−261.
6. Toyoshima, C., Nakasako, M., Nomura, H., and Ogawa, H. (2000) *Nature 405*, 647−655.
7. Geering, K. (1990) *J. Membr. Biol. 115*, 109−121.
8. Gottardi, C. J., and Caplan, M. J. (1993) *J. Biol. Chem. 268*, 14342−14347.
9. Skrabanja, A. T., De Pont, J. J., and Bonting, S. L. (1984) *Biochim. Biophys. Acta 774*, 91−95.
10. Rabon, E. C., McFall, T. L., and Sachs, G. (1982) *J. Biol. Chem. 257*, 6296−6299.
11. Blostein, R., Dunbar, L. A., Mense, M., Scanzano, R., Wilczynska, A., and Caplan, M. J. (1999) *J. Biol. Chem. 274*, 18374−18381.
12. Dunbar, L. A., Aronson, P., and Caplan, M. J. (2000) *J. Cell Biol. 148*, 769−778.
13. Polvani, C., and Blostein, R. (1988) *J. Biol. Chem. 263*, 16757−16763.
14. Polvani, C., Sachs, G., and Blostein, R. (1989) *J. Biol. Chem. 264*, 17854−17859.
15. Mense, M., Dunbar, L. A., Blostein, R., and Caplan, M. J. (2000) *J. Biol. Chem. 275*, 1749−1756.
16. Jorgensen, P. L., and Petersen, J. (1982) *Biochim. Biophys. Acta 705*, 38−47.
17. Ottolenghi, P. (1975) *Biochem. J. 151*, 61−66.
18. Jeanmougin, F., Thompson, J. D., Gouy, M., Higgins, D. G., and Gibson, T. J. (1998) *Trends Biochem. Sci. 23*, 403−405.
19. Guex, N., and Peitsch, M. C. (1997) *Electrophoresis 18*, 2714−2723.
20. Peitsch, M. C. (1996) *Biochem. Soc. Trans. 24*, 274−279.
21. Rice, W. J., Young, H. S., Martin, D. W., Sachs, J. R., and Stokes, D. L. (2001) *Biophys. J. 80*, 2187−2197.
22. Vilsen, B. (1995) *FEBS Lett. 363*, 179−183.
23. Harris, S. L., Perlin, D. S., Seto-Young, D., and Haber, J. E. (1991) *J. Biol. Chem. 266*, 24439−24445.
24. Doyle, D. A., Morais Cabral, J., Pfuetzner, R. A., Kuo, A., Gulbis, J. M., Cohen, S. L., Chait, B. T., and MacKinnon, R. (1998) *Science 280*, 69−77.
25. Hinton, J. F., Fernandez, J. Q., Shungu, D. C., Whaley, W. L., Koeppe, R. E. D., and Millett, F. S. (1988) *Biophys. J. 54*, 527−533.
26. Urry, D. W., Prasad, K. U., and Trapane, T. L. (1982) *Proc. Natl. Acad. Sci. U.S.A. 79*, 390−394.
27. Koenderink, J. B., Hermsen, H. P., Swarts, H. G., Willems, P. H., and De Pont, J. J. (2000) *Proc. Natl. Acad. Sci. U.S.A. 97*, 11209−11214.
28. Koenderink, J. B., Swarts, H. G., Stronks, H. C., Hermsen, H. P., Willems, P. H., and De Pont, J. J. (2001) *J. Biol. Chem. 276*, 11705−11711.
29. Sachs, J. R. (1987) *J. Gen. Physiol. 90*, 291−320.
30. Jewell-Motz, E. A., and Lingrel, J. B. (1993) *Biochemistry 32*, 13523−13530.
31. Kuntzweiler, T. A., Wallick, E. T., Johnson, C. L., and Lingrel, J. B. (1995) *J. Biol. Chem. 270*, 2993−3000.
32. Vilsen, B. (1992) *FEBS Lett. 314*, 301−307.
33. Vilsen, B. (1997) *Biochemistry 36*, 13312−13324.
34. Vilsen, B. (1995) *Biochemistry 34*, 1455−1463.
35. Grishin, A. V., Sverdlov, V. E., Kostina, M. B., and Modyanov, N. N. (1994) *FEBS Lett. 349*, 144−150.

BI025819Z